Actual trends in development of Power System Relay Protection and Automation
1–5 June 2015, Sochi (Russia)

Hierarchically Coordinated Protection: An Integrated Concept of Corrective, Predictive, and Inherently Adaptive Protection

M. KEZUNOVIC, P.-C. CHEN, A. ESMAEILIAN, M. TASDIGHI
Texas A&M University
United States of America
kezunov@ece.tamu.edu

KEYWORDS

Cascading event, data analytics, data correlation, distributed generation, geospatial analysis, outage management, power system protection, support vector machine.

1 INTRODUCTION

This paper relates to a new protection paradigm where corrective, adaptive and predictive relaying features are introduced.

The value of *corrective relay operation* can be assessed by looking at the situations when relay mis-operations occur. Analysis of recent historical blackouts has revealed that the power system catastrophic events happened following consecutive cascading events such as transmission line outages, overloads and malfunctions of protective relays [1]-[3]. In general, cascade events can be divided into two time stages. In the first stage, successive events are slow enough to be analyzed as steady-state. If no action occurs to restore the grid to the normal operation condition, and meanwhile several major disturbances occur causing fast transient stability violation, a system collapse will happen. This stage is named as second or irreversible stage. Early prediction and proper control actions during the first stage can prevent further unfolding of cascade events.

When a transmission line is tripped due to the operation of protective relays, a relay mis-operation detection tool can confirm whether the relay operation was correct or the transmission line was healthy and incorrectly tripped [4]. The advantages of such tool could be itemized as higher reliability and redundancy, faster restoration and enhanced critical decision making during disturbances [5]. This tool can also support the reliable implementation of new applications such as transmission line switching (topology) control [6].

The value of *adaptive relay operation* [7]-[10] may be assessed by looking at the situations where adaptive features are desirable. So far, the protection challenges raised by DG integration in the system have been mostly looked at from the distribution side. However, with high penetration of DGs in the network, the protection concerns extend to transmission level also. According to the literature [11]-[12], one of the challenges that high levels of DG penetration create for the power transmission system protection is unintended bulk DG tipping following a disturbance in the transmission system. The interaction of system dynamics with sensitive control and protection measures which are necessary, according to IEEE standards, to prevent or minimize the existence of an inadvertent island, could lead to unintended tripping of DG. For example, if a short-circuit takes place in the transmission grid and its effects on voltage are propagated downstream to the distribution level, it may provoke the disconnection of a large amount of DG. Since these DG plants are tripped, a sudden increase in power flow coming from upstream takes place in this network area. This may provoke cascading operation of distance relays in transmission lines as a result of overload situations.

Fig. 1 shows the impedance trajectory seen by a relay in the vicinity of DG bus when 500 MW of DG is tripped following a three phase fault in the transmission level in New England 39 bus system. As it could be seen, the DG tripping has pushed the impedance trajectory into third zone of the relay in the vicinity of the DG bus and might lead to the relay false tripping.

The value of *predictive relay operation* may be assessed by looking at the situations where occurrence of faults may be predicted based on historical data. Weather factors are primarily responsible for the outages [13]. The severity of weather is predicted to become progressively worse [14]. The operation of electrical systems, particularly in an overhead structure, is very sensitive to the weather conditions. Therefore, it is imperative to come up with corresponding strategies. One of the promising solutions is to have a way of implementing weather-aware protection in a predictive manner. It is shown that the application of weather data may bring additional benefits to the outage management [15]-[16].

The question of how to correlate weather data from various sources with power system data remains a challenge. Such correlation requires the ability to leverage the geospatial nature of predictive information. In this case, utilizing Geographical Information System (GIS) is the key for correlating different layers of data for geospatial analysis. Within the traditional concept of utility, GIS is defaulted as a visualizing mapping tool. Yet, the spatial-temporal information can render not only the geographical visualizations but interpretation of different data layers. The flow of data provides useful knowledge extraction which enables better decision-making process for a utility operator. Further study is needed how this information may be utilized to develop predictive protection strategy

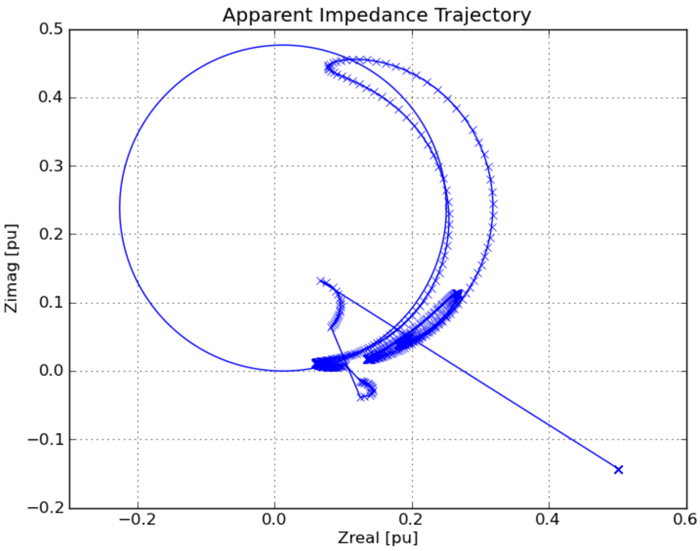

Figure 1: The apparent impedance trajectory for a scenario of DG tripping following a three phase fault clearing

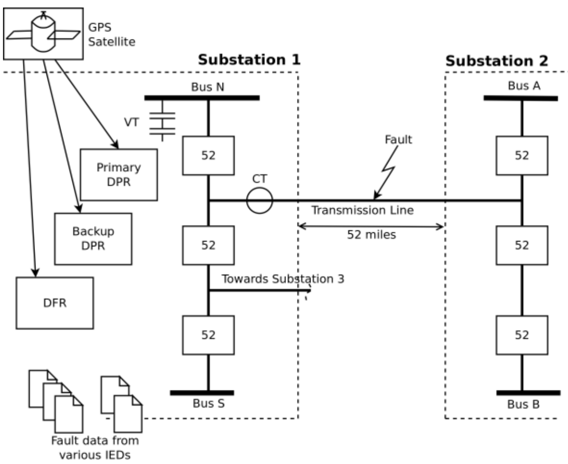

Figure 2: Typical transmission line setup with measurements from both ends

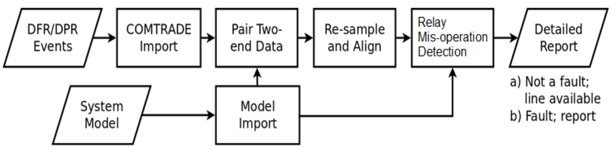

Figure 3: Automated analysis of time-synchronized event data

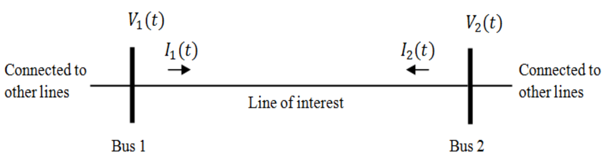

Figure 4: Transmission line with two-end measurements

2 EXAMPLES OF TECHNIQUES USED TO SOLVE THE PROBLEM

2.1 Relay mis-operation detection tool (example of corrective relaying strategy)

Fig. 2 depicts a typical transmission line setup with the event-triggered measurements from both ends. As it can be seen, the line can be monitored by different substation IEDs at both ends (details are only shown in substation 1). When a fault (or disturbance seen as a fault by the protective device) occurs, several IEDs can be triggered and they will capture event measurements. The assumption is that the data samples are synchronized and time-stamped using the Global Positioning System (GPS), and a high-speed communication link between substations and control center is available. The relay mis-operation detection tool implementation is illustrated in Fig. 3. Following is the description of each step.

Step 1. DFR/DPR Events Import: The required IED device data consists of voltage and current samples captured by DFR or DPR. The fault data and system model data are necessary inputs for the tool to run and operate correctly and accurately. The involved DFR and DPR devices varied by vendor, types, and vintage. All data files from different vendors have been converted in unified COMTRADE file format (IEEE C37.111-1999).

Step 2. System Model Import: The system model topology is obtained from the PSS/E (*.raw) file and used for pairing the event files coming from two ends of the same transmission line.

Step 3. Pairing the Two-end Data: There can be multiple IED files created during a disturbance at different substations. Utilizing the network topology from the system model, the IED files from the neighboring nodes are paired to extract the two-end measurement data corresponding to the transmission line between the buses.

Step 4. Re-sample and Align: After the two-end data are paired, they are processed in order to extract data samples for instantaneous voltage and current signals measured at both ends of the line. The extracted data samples are re-sampled and aligned (when the triggering time was not the same) in order to obtain the same sampling rate at both ends as well as synchronized samples.

Step 5. Relay mis-operation detection: The relay mis-operation detection tool core algorithm has been introduced in [17], [18]. Here, we provide an overview of relay mis-operation detection core algorithm implemented as a part of the proposed tool. In Fig. 4, $V_1(t)$ and $I_1(t)$ represents voltage and current measured at one end (Bus 1) of the line at instance t. Similarly $V_2(t)$ and $I_2(t)$ represents voltage and current measured at the other end (Bus 2) of the line. Instantaneous powers calculated at both ends are:

$$P_1(t) = V_1(t) \times I_1(t) \quad , \quad P_2(t) = V_2(t) \times I_2(t) \tag{1}$$

During the normal operation, $P_1(t)$ and $P_2(t)$ will be in phase opposition to each other for the current directions assumed. However, for the faulty phases, when the fault is initiated, they will be in-phase with each other. For un-faulted phases the phase opposition will be maintained even after the fault inception. If a load level change or a fault in neighboring line occurs, the calculated instantaneous powers will remain in opposite direction. Therefore, the method can discriminate load level changes or external faults from internal ones. To represent this feature mathematically, we use signum function which is defined as:

$$\operatorname{sgn}(x) = \begin{cases} -1, & x < 0 \\ 0, & x = 0 \\ 1, & x > 0 \end{cases} \tag{2}$$

We calculate $\operatorname{sgn}(P_1(t))$ and $\operatorname{sgn}(P_2(t))$ and plotted the difference for each phase.

$$P\operatorname{sgn}(t) = \operatorname{sgn}(P_1(t)) - \operatorname{sgn}(P_2(t)) \tag{3}$$

Theoretically, before a fault has been initiated, this difference $P\operatorname{sgn}(t)$ should be ±2 and after fault occurrence $P\operatorname{sgn}(t)$ should be 0 on all faulty phases. We used the change of difference of $\operatorname{sgn}()$ to detect fault instant as (3). However, due to transients and noise in the measurements, some outliers exist. To avoid incorrect decisions caused by outliners, a moving window of 5 ms is used to check whether at least 80% of $P\text{sgn}(t)$ are zero, which indicates a fault.

Step 6. Detailed Report: The results of relay mis-operation detection tool are provided in the form of detailed analysis report. As shown in Fig. 3, the outcome of the analysis may be: a) no fault, which means that the tripped line may be available to switch back in; b) fault detected and operation of relay has been confirmed, which means no need for a corrective action.

2.2 Support Vector Machine Based Protection Scheme (example of adaptive relaying strategy)

Recently, supervised learning techniques have attracted attention in various power system disturbance analysis studies such as power swing detection and fault detection and classification. Among these techniques, Support Vector Machine (SVM) is shown to be an accurate and easy to train method. SVM is a learning method based on the statistical learning theory. In this method, the idea is to map the original input space into a high-dimensional dot product space which is called a feature space, and determine the hyper-plane in the feature space to maximize the generalization ability of the classifier. The optimal hyper-plane is found by deploying the optimization theory, and respected insights provided by the statistical learning theory.

Implementing SVM method involves separating the data into two categories: training and testing data sets. These sets include instances each of which contains a label (target value) and multiple features (observed variables). The SVM goal is to create a model based on the training data sets which could predict the labels for the test data sets if the features of the test data sets are given to the model.

In this study a SVM based protection scheme is proposed which enables the relay to detect a DG tripping case from faults. The output of the SVM module and the distance relay pick-up signal together identify the trip signal as shown in Fig. 5. Proper input features for the SVM could be chosen from the principal component analysis [19]. The input feature vector includes the following measurements at the relay installation point: the bus voltage, branch current, active and reactive power flows. The following are the steps of implementing the proposed algorithm:

Step 1. Instances preparation:
Simulation of multiple DG tripping cases with different parmeters: fault location, DG tripped capacity, and DG tripping instant.

Step 2. Feature extraction:
Monitoring and recording the features extracted by principal component analysis (PCA).

Step 3. Training set data preparation:
Randomly choosing the training set out of all the simulated instances.

Step 4. Kernel parameter selection:
Having chosen RBF kernel function, the cross-validation technique is implemented to obtain the proper kernel parameters in training the SVM.

Step 5. SVM training:
Train the SVM based on the obtained kernel parameters.

Step 6. SVM testing:
Test the SVM for the testing data set, i.e. the instances not chosen as training instances.

2.3 Weather Impacts on Outage Management (example of a predictive relaying strategy)

Vegetation contact on distribution lines is one of the most common fault types. The fall of tree limbs and trunks are due to the large wind. An example provided examines the utilization of GIS for outage prediction in the context of faults caused by the lack of tree-trimming. This requires an understanding how typical power system data is correlated with the GIS containing the wind and canopy height data. These sources are used as inputs to generate outage vulnerability assessment for different geographic areas, and then correlate it with feeder data for outage mapping. In general, data used for this types of analysis must be properly chosen and processed for specific application purposes. The data sources will be shown first, and then an example correlation will be demonstrated using a GIS platform named ArcGIS [20].

The power system data used in this example is extracted from the Storm Vulnerability Assessment tutorial from Esri [21]. The components utilized are primary overhead feeders.

The wind forecast data is from National Digital Forecast Database (NDFD) [22]. The data can be accessed through graphical user interface (GUI) (named "tkdegrib") provided by NDFD and then converted to Shapefiles (polygon data format) for further processing in ArcGIS [23].

The canopy height data used in the analysis is the three dimensions Global Vegetation Map [24], [25]. The data format is raster at 1 km resolution using data from the Geoscience Laser Altimeter System (GLAS) aboard Ice, Cloud, and land Elevation Satellite (ICESat) [25]. The average canopy height in each grid cell is recorded.

In the example, the process of data correlation is presented below.

Step 1. Process Vegetation Data
The vegetation data were masked to obtain the grid cells containing the area for just the distribution network.

Step 2. Process Wind Data
The wind polygon data were clipped to match the processed vegetation polygon.

Step 3. Correlate vegetation and wind data and then perform the vulnerability analysis
The data from the wind polygon were spatially joined with the vegetation polygons. This resulted in each cell containing both canopy height and wind data which allows for analysis given a set of rules - e.g., wind speed will be taken into consideration first prior to the canopy height data. Each grid cell is then labeled for prioritizing in the outage search sequences.

Step 4. Identify the system components in each area and output results
It should be noted that one component (e.g. a line) may stretch across multiple polygons or grid areas (i.e. not just inside a single area). While correlating other data layers with power system data layer, the power system must be divided into different areas where components may be separated into multiple pieces to account for this.

By correlating the different data layers, the region with high wind speed and large canopy height data could be identified as the potential outage area.

3 RESULTS AND BENEFITS

3.1 Relay mis-operation detection tool (example of a corrective relay tool)

The relay mis-operation detection tool has been tested against various simulated and field data test cases. The following two examples demonstrate how the tool behaves in the case of a fault as well as relay mis-operation. In both cases, the sampled data are taken from actual IED device in field.

As shown in Fig. 6 (a-c), the instantaneous powers from two ends at phase B and C are in the opposite direction before and after disturbance. While in phase A, the direction has been changed after fault initiation time. As a result, the output of the relay mis-operation detection tool reports "phase A to ground fault". Fig. 6 (d-f) depicts plot of $P\mathrm{sgn}(t)$ with respect to the time for three phases. It can be seen that in phases B and C less than 80% of the total samples are zero. However, more than 80% of the total samples of phase A is zero.

Fig. 7 shows the same type of output plots for a relay mis-operation test case. Fig. 7 (a-c) depicts instantaneous power $P_1(t)$ and $P_2(t)$ calculated based on data captured by DFR units at the two ends of transmission line with respect to time. In this case, the information received by utility shows

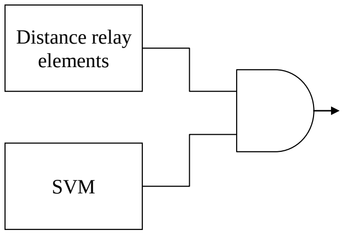

Figure 5: Proposed scheme block diagram

that the fault occurred on a neighboring line. There has been falsely tripped due to single phase fault (ag) while the later investigation of the case reveals that the relay mis-operates due to a single phase fault on an adjacent line.

From Fig. 7 (a-c) one can observe that the opposite direction of instantaneous powers from two ends stay the same before and after disturbance. As a result, the output of the tool indicates “no fault” condition. Fig. 7 (d-f) shows plot of $P\mathrm{sgn}(t)$ with respect to time for three phases. It can be seen that less than 80% of the total samples are zero which means no fault has been detected in any of three phases.

3.2 Support Vector Machine Based Protection Scheme (example of an adaptive relay tool)

In this study, the SVM is trained for unintended DG tripping scenarios in New England 39 bus system. To train the SVM, multiple instances have been simulated which include: fault on multiple points along the third zone of the target relay, various DG tripping capacity, and multiple DG tripping instants following the fault. The input vector for the SVM includes the difference of feature values with those of previous cycle. The sampling rate is considered 10 samples per cycle. Considering multiple scenarios for creating the data sets, 25000 instances of DG tripping cases and faults are provided. 15000 instances are chosen randomly as training data sets and the rest as the testing ones.

In the next step, a proper Kernel function and its corresponding parameters should be chosen and determined to train the SVM. For this purpose radial basis kernel function (RBF) is deployed. RBF kernel needs two parameters to be determined: C and γ. The C and γ values, which are best for a given problem, are not known beforehand; so, a parameter search should be done. The values which enable the SVM to predict the testing data sets accurately are desired. As mentioned above, the data is divided into two sets one of which is considered unknown. To examine of SVM performance more precisely, the prediction accuracy for the unknown set has a key role as it could be considered as an independent data set. The cross-validation technique [26] is used as an improved version of the search procedure for determining C = 32768 and γ = 32 for the RBF kernel. It was seen that the SVM reaches the accuracy of 93.7% with the selected kernel parameters. Therefore, the SVM detects the DG

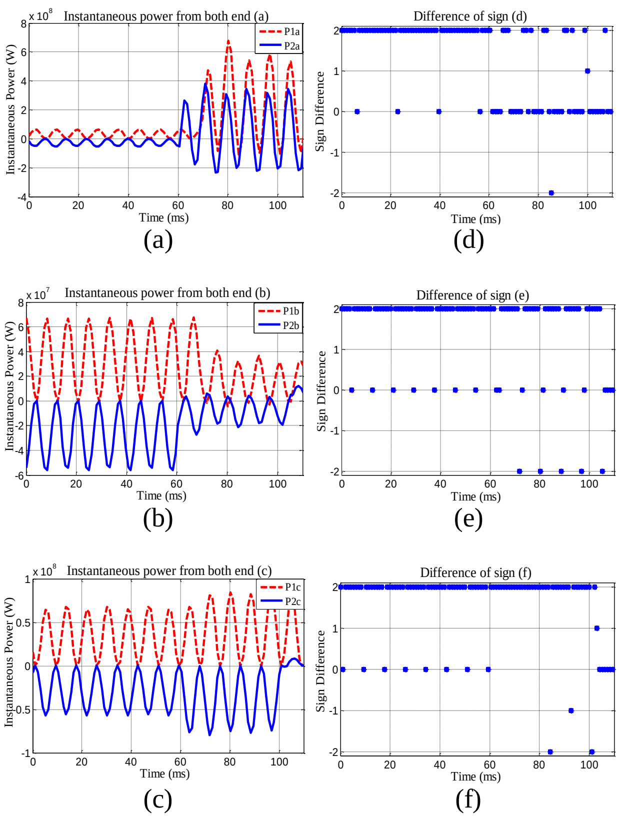

Figure 6: Single phase to ground fault detection and classification

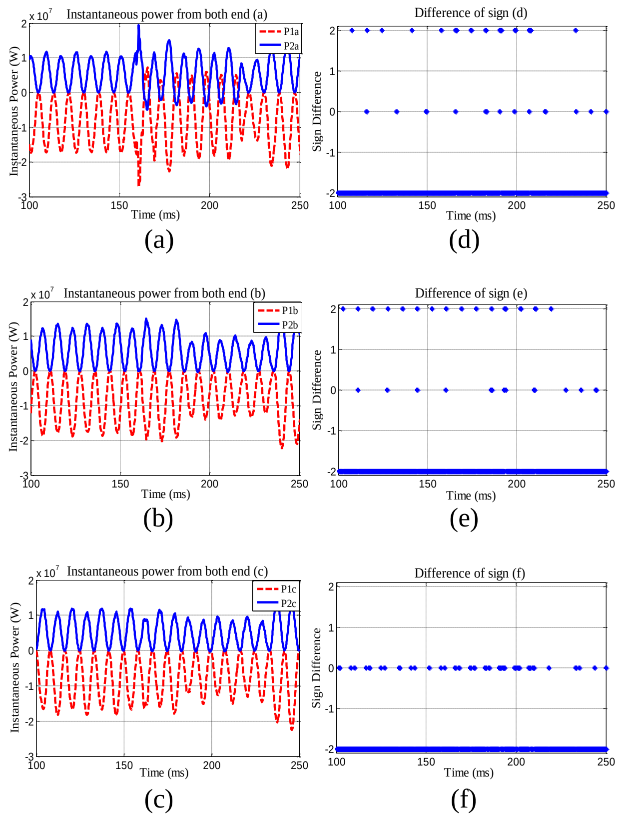

Figure 7: Relay Mis-operation Detection

tripping cases with a high precision which prevents the relay miss-operation and probable cascading failures on such unintended bulk DG tripping cases.

The other advantage of the proposed protection scheme is that it could be implemented in combination with other additional protection schemes such as power swing blocking and that way help maintain the power system protection dependability and security effectively.

3.3 Weather Impacts on Outage Management (example of a predictive relay tool)

Fig. 8 shows the final results from this example. Fig. 8 (a) shows the power system and wind data layers where the larger wind speed is at the right hand side. Fig. 8 (b) shows the power system and canopy height data where different saturation levels of green color represent different height of canopy. Fig. 8 (c) shows the result of combining each of these layers together. Based on the wind and canopy data, the first three areas should be searched by the dispatched crews are labeled in Fig. 8 (c).

The example discussed here is intended for the prediction purposes but can be also applied to real-time operations stages (search for outages with insufficient outage report information). In the reality, the localized nature of weather conditions (e.g. various types of storms) means that the process for corresponding types of outages may be very different than what is described in the basic example provided here. The rules used to characterize risk or response priority should be based on real conditions and past experience.

The selections of input data are critical for the data correlation provided here. The level of attribute detail provided has critical impacts on the model results. For example, Fig. 9 shows the wind data from reference [27] with the Kriging function in Geostatistical Analyst in ArcGIS. Kriging is a technique for interpolating predicting values of location with no measurement data. In Fig. 9, there are only 4 data points which do not render very effectively adjacent polygons for further analysis. As shown, the area where the network intersects is not reasonably subdivided.

Similarly, the wind speed data downloaded from the live feeds of NDFD [28] contain only 4 data points. The layer file does not contain additional attribute information which can be used for further processing. These data simply visualize wind speeds, and are not readily usable.

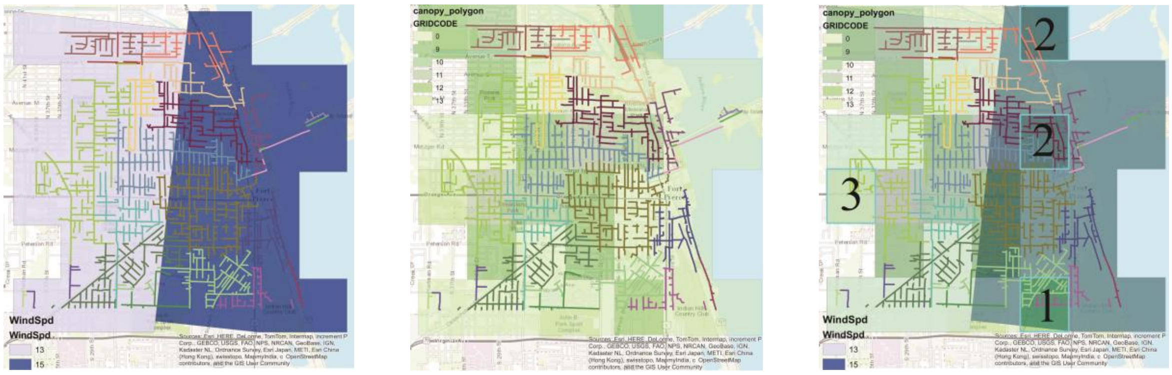

(a) (b) (c)

Figure 8: Data layer correlations. (a) Power system and wind data. (b) Canopy height and power system data. (c) All three layers of data

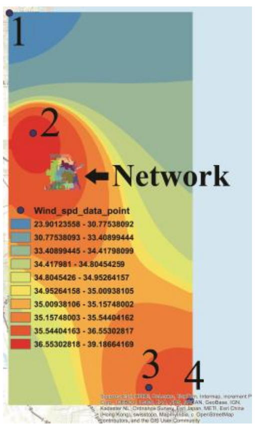

Figure 9: Only 4 data points available from [22] for kriging

4 CONCLUSION

Based on the discussions in the paper the following conclusion can be reached:

- Corrective, adaptive and predictive relay features are feasible
- Such protection paradigm has distinct benefits but requires additional data or equipment
- The test results illustrate the robustness of the solutions
- The practical use of such a protection paradigm is yet to be fully explored
- Future steps are needed to identify other applications that may benefit from such a paradigm

REFERENCES

[1] M. Johnson, "Line Protection and Power System Collapse," Master's Thesis, Department of Electric Power Engineering, Chalmers University of Technology, Goteborg, Sweden, 2001.
[2] "Final Report on the August 14, 2003 Blackout in the United States and Canada: Causes and Recommendations," U.S.-Canada Power System Outage Task Force, Apr. 2004.
[3] R. Baldick et al., "Initial Review of Methods for Cascading Failure Analysis in Electric Power Transmission Systems," IEEE PES General Meeting, Pittsburgh, PA, USA, Jul. 2008.
[4] M. Kezunovic, S. Meliopoulos, V. Venkatasubramanian, and V. Vittal, Application of Time-Synchronized Measurements in Power System Transmission Networks, New York: Springer, 2014.
[5] T. Popovic and M. Kezunovic, "Measures of value: data analytics for automated fault analysis," IEEE Power & Energy Magazine, vol. 10, no. 5, pp 58-69, Sep. 2012.
[6] M. Kezunovic et al., "Reliable Implementation of Robust Adaptive topology Control," HICCS Hawaii International Conference System Science, Manoa, Hawaii, Jan. 2014.
[7] G. D. Rockefeller, et al., "Adaptive transmission relaying concepts for improved performance," IEEE Trans. Power Del., vol. 3, no. 4, pp. 1446-1458, Oct. 1988.
[8] J. D. Codling, et al., "Adaptive relaying. A new direction in power system protection," IEEE Potentials, vol. 15, no. 1, pp. 28-33, Feb./Mar. 1996.
[9] J.-A. Jiang, et al., "A novel adaptive PMU-based transmission-line relay-design and EMTP simulation results," IEEE Trans. Power Del., vol. 17, no. 4, pp. 930-937, Oct. 2002.
[10] J. Upendar, et al., "Comprehensive Adaptive Distance Relaying Scheme for Parallel Transmission Lines," IEEE Trans. Power Del., vol. 26, no. 2, pp. 1039-1052, Apr. 2011.
[11] J. A. Peças Lopes, et al., "Integrating distributed generation into electric power systems: A review of drivers, challenges and opportunities," Elect. Power Syst. Res., vol. 77, no. 9, pp. 1189–1203, Jul. 2007.
[12] R. A. Walling and N. W. Miller, "Distributed generation islanding-implications on power system dynamic performance," IEEE/PES Summer Meeting, vol. 1, pp. 92-96, Jul. 2002.
[13] Executive Office of the President, "Economic Benefits of Increasing Electric Grid Resilience to Weather Outages," Aug. 2013.
[14] A. B. Smith and R. W. Katx, "US billion-dollar weather and climate disasters: data sources, trends, accuracy and biases," Natural Hazards, vol. 67, no. 2, pp. 387-410, Jun. 2013.
[15] M. Kezunovic, et al., "The role of big data in improving power system operation and protection," Int. Inst. for Research and Education in Power Syst. Dynamics Symp. (IREP), Aug. 2013.
[16] P.-C. Chen, et al., "The Use of Big Data for Outage Management in Distribution Systems," Int. Conf. on Electricity Distrib. (CIRED), Jun. 2014.
[17] P. Dutta, A. Esmaeilian, and M. Kezunovic, "Transmission-Line Fault Analysis Using Synchronized Sampling," IEEE Trans. Power Del., vol. 29, no. 2, Apr. 2014.
[18] A. Esmaeilian, M. Kezunovic, "Evaluation of Fault Analysis Tool under Power Swing and Out-of-Step Conditions," 46th North American Power Symposium (NAPS), Sep. 2014.
[19] K. Fukunaga, Introduction to Statistical Pattern Recognitions. New York: Academic Press, 1972.
[20] ArcGIS, Esri. [Online] Available: https://www.arcgis.com/features/
[21] Storm Vulnerability Assessment, ArcGIS for Utilities, Esri. [Online] Available: http://solutions.arcgis.com/utilities/electric/help/storm-vulnerability/
[22] General Information, NDFD, NWS. [Online] Available: http://ndfd.weather.gov/index.htm
[23] National Digital Forecast Database (NDFD) Tkdegrib and GRIB2 DataDownload and ImgGen Tool Tutorial Access Data, NDFD, NWS. [Online] Available: http://ndfd.weather.gov/technical.htm
[24] 3D Land Mapping, Jet Propulsion Laboratory, California Institute of Techonology. [Online] Available: http://lidarradar.jpl.nasa.gov/
[25] M. Simard, et al., "Mapping forest canopy height globally with spaceborne LIDAR," J. Geophysical Research, vol. 116, G04012, pp. 1-12, Nov. 2011.
[26] C. C. Chang and C. J. Lin. "LIBSVM: a library for support vector machines," ACM Transactions on Intelligent Systems and Technology, vol. 2, no. 3, Apr. 2011.
[27] Data Files and Feeds, SECOORA. [Online] Available: http://secoora.org/data/data_feeds
[28] Folder: LiveFeeds, ArcGIS REST Services Directory. [Online] Available: http://tmservices1.esri.com/arcgis/rest/services/LiveFeeds